Correcting Liquefaction Resistance for Aged Sands Using Measured to Estimated Velocity Ratio

Ronald D. Andrus[1]; Hossein Hayati[2]; and Nisha P. Mohanan[3]

Abstract: Factors for correcting liquefaction resistance for aged sands using ratios of measured to estimated shear-wave velocity (MEVR) are derived in this paper. Estimated values of shear-wave velocity (V_S) are computed for 91 penetration resistance-V_S data pairs using previously published relationships. Linear regression is performed on values of MEVR and corresponding average age. Age of the sand layer is taken as the time between V_S measurements and initial deposition or last critical disturbance. It is found that MEVR increases by a factor of about 0.08 per log cycle of time, and time equals about 6 years on average when MEVR equals 1 for the recommended penetration resistance-V_S relationships. The resulting regression equation is combined with the strength gain equation reported by Hayati et al. 2008 in "Proc., Geotechnical Earthquake Engineering and Soil Dynamics IV," to produce a MEVR versus deposit resistance correction relationship. This new corrective relationship is applied to create liquefaction resistance curves based on V_S, standard penetration test blow count, and cone tip resistance for sands of various ages (or MEVRs). Because age of natural soil deposits is usually difficult to accurately determine, MEVR appears to be a promising alternative.

DOI: 10.1061/(ASCE)GT.1943-5606.0000025

CE Database subject headings: Aging; Sand; Cone penetration tests; Earthquakes; In situ tests; Soil liquefaction; Wave velocity; Penetration tests.

Introduction

The simplified procedure originally proposed by Seed and Idriss (1971) is commonly used throughout the world to evaluate the resistance of soil to liquefaction. In this simplified procedure, the resistance of soil to liquefaction is expressed in terms of a variable called the cyclic resistance ratio (CRR) and the cyclic loading on the soil caused by the earthquake is expressed in terms of a variable called the cyclic stress ratio (CSR). Liquefaction is predicted to occur if CSR $\geq$ CRR. Semiempirical charts based on the standard penetration test (SPT) blow count, the cone penetration test (CPT) tip resistance, or the small-strain shear wave velocity (V_S) are typically used to estimate CRR. A limitation of the CRR charts is that they were derived from field case histories involving soil deposits less than a few thousand years old and there is no generally accepted procedure for applying them to older soil deposits (Youd et al. 2001).

Youd and Perkins (1978) noted that soil deposits $<$500 years old generally have high to very high susceptibility to liquefaction, whereas older Holocene-age ($<$10,000 years) sediments have moderate to high susceptibility and Pleistocene-age (10,000 to 1.8 million years) sediments have very low to low susceptibility. Efforts to quantify the influence of age on liquefaction resistance have involved laboratory cyclic triaxial tests (Seed 1979; Troncoso et al. 1988), laboratory cyclic triaxial and field tests (Arango and Migues 1996; Arango et al. 2000; Robertson et al. 2000; Lewis et al. 2004), and field tests at sites that did and did not liquefy during earthquakes (Lewis et al. 1999; Hayati and Andrus 2008). A summary of these previous efforts to quantify the influence of age on CRR is presented in Hayati et al. (2008).

It has been suggested that an age correction factor be applied to CRR as follows (Arango et al. 2000; Lewis et al. 2004; Andrus et al. 2004b):

$$\mathrm{CRR}_K = \mathrm{CRR}\ K_{\mathrm{DR}} \tag{1}$$

where CRR_K=cyclic resistance ratio corrected for age and cementation; and K_{DR}=factor to correct for influence of age and cementation on deposit resistance. For estimating K_{DR}, Hayati et al. (2008) critically reviewed previous studies and suggested the following relationship:

$$K_{\mathrm{DR}} = 0.17 \log_{10}(t) + 0.83 \tag{2}$$

where t=time since initial soil deposition or last critical disturbance (e.g., liquefaction). It should be noted that Eq. (2) plots significantly below the corrective relationship suggested by Arango et al. (2000), but exhibits a similar slope. It should also be noted that Eq. (2) was derived using penetration resistance directly (i.e., without age correction) and assuming the commonly used CRR curves as reference. A limitation of Eq. (2) is that it is usually difficult to accurately determine t in natural soil deposits. In addition, the effect of cementation on deposit resistance may not be included in t.

A promising alternative to estimating age of a soil deposit is the ratio of measured V_S to V_S estimated from SPT or CPT resistances. Andrus et al. (2007) originally called this ratio the age scaling factor. However, because there are factors other than age

[1]Associate Professor, Dept. of Civil Engineering, Clemson Univ., Clemson, SC 29634-0911 (corresponding author). E-mail: randrus@clemson.edu

[2]Graduate Research Assistant, Dept. of Civil Engineering, Clemson Univ., Clemson, SC 29634-0911.

[3]Project Geotechnical Engineer, Golder Associates Inc., Mt. Laurel, NJ 08054; formerly, Graduate Research Assistant, Dept. of Civil Engineering, Clemson Univ., Clemson, SC 29634-0911.

Note. This manuscript was submitted on February 13, 2008; approved on September 16, 2008; published online on May 15, 2009. Discussion period open until November 1, 2009; separate discussions must be submitted for individual papers. This paper is part of the ***Journal of Geotechnical and Geoenvironmental Engineering***, Vol. 135, No. 6, June 1, 2009. ©ASCE, ISSN 1090-0241/2009/6-735–744/$25.00.

Table 1. Data from Holocene Sands with FC < 20% and $I_c < 2.25$ [Modified from Andrus et al. (2004a)]

Site name	Depth (m)	USCS soil type	D_{50} (mm)	FC[a] (%)	V_S test type[b]	V_{S1} (m/s)	$(V_{S1})_{cs}$ (m/s)	$(N_1)_{60cs}$	I_c	q_{t1N}	$(q_{t1N})_{cs}$	Approximates average age[e] (years)
California, USA												
Bay Bridge, SFOBB1	5.4–7.2	SP-SM	0.26	12	CH	151	152	7	2.15	43	67	2.2 (L)
Bay Bridge, SFOBB1	8.0–9.9	SP-SM	0.27	8	CH	150	151	20	1.90	65	77	2.2 (L)
Bay Farm Island-Dike	3.7–7.8	SP-SM	0.25	11	CH	231	237	50	1.85	201	230	15 (NL)
Port of Oakland, P007-2	3.0–5.1	SP-SM	0.29	7	CH/SCPT	182	183	22	1.50	173	173	2.2 (L)
Port of Oakland, P007-2	5.3–6.8	SP-SM	0.30	6	CH/SCPT	172	172	13	1.88	63	73	2.2 (L)
Port of Oakland, P007-2	6.8–9.1	SP-SM	0.30	3	CH/SCPT	167	167	16	1.71	107	112	2.2 (L)
State Beach, UC-15	2.0–3.8	SP	0.28	2	SCPT	137	137	7	1.90	56	67	4.8 (L)
State Beach, UC-16	2.4–4.6	SP	0.43	2	SCPT	192	192	22	1.47	171	171	4.8 (L)
State Beach, UC-16	4.6–6.7	SP	0.57	1	SCPT	175	175	17	1.40	166	166	4.8 (L)
Treasure Island, B1-B3	2.2–4.0	SP-SM	0.21	7	CH	162	162	21	1.87	73	85	2.2 (L)
Treasure Island, B1-B3	9.0—11.5	SM	0.21	14	CH	180	183	17	2.11	43	64	2.2 (L)
Treasure Island, UM-05	3.3–5.7	SP	0.33	4	SCPT	170	170	14	1.82	70	79	1.7 (L)
Treasure Island, UM-06	2.2–5.0	SP	na[c]	3	SCPT	175	175	12	2.10	30	44	1.7 (L)
Treasure Island, UM-09	2.7–6.3	SP-SC	0.15	11	SCPT	160	161	9	2.04	50	68	1.7 (L)
Canada												
Fraser River Delta, Kidd	12.0–17.0	SP	0.20	<5	SCPT	177	177	13	<1.64[d]	68	68	4,000 (NL)
Fraser River Delta, Massey	8.0–13.0	SP	0.20	<5	SCPT	168	168	10	<1.64[d]	53	53	200 (NL)
HVC Mine, LL Dam	6.0–10.0	SP-SM	0.25	8	SCPT	153	154	5	1.79[d]	39	43	5 (NL)
HVC Mine, Highmont Dam	8.0–12.0	SP-SM	0.25	10	SCPT	141	142	6	1.88[d]	44	52	15 (NL)
Syncrude, J-Pit	3.0–7.0	SM	0.17	15	SCPT	127	129	6	2.07[d]	20	28	0.17 (NL)
Syncrude, Mildred Lake	27.0–37.0	SP-SM	0.16	10	SCPT	156	157	19	1.88[d]	74	87	12 (NL)
Japan												
Hakodate Port No. 1	8.5–11.4	SP-SM	0.24	7	SL	149	149	7	1.99	48	62	1.0 (L)
Kushiro Port, No. 2 (PB-1)	3.5—5.5	SP-SM	0.17	7	SL	195	196	25	na	na	na	0.67 (L)

[a]FC=fines content (silt and clay).

[b]CH=crosshole; SCPT=seismic CPT; SL=suspension logger.

[c]na=not available.

[d]Estimated I_c from: $FC = 1.75 I_c^{3.25} - 3.7$ for $1.26 < I_c < 3.5$ (Robertson and Wride 1998).

[e]Time between deposition (or liquefaction) and V_S measurements; L=known liquefaction; and NL=no known liquefaction.

that influence this ratio, it is herein called the measured to estimated V_S ratio (MEVR). The purpose of this paper is to develop a relationship between MEVR and $\log_{10}(t)$, and use this relationship with Eq. (2) to produce CRR curves corrected for aging effects. The relationship between MEVR and $\log_{10}(t)$ is derived for the first time in this paper using CPT-V_S and SPT-V_S data pairs from sand deposits of known age.

Database

The general criteria used for selecting the penetration resistance-V_S data pairs are as follows (Piratheepan 2002; Ellis 2003; Mohanan 2006): (1) measurements are from below the groundwater table and where reasonable estimates of effective stress can be easily made; (2) measurements are from thick, uniform sand layers identified using primarily the CPT profiles; (3) CPT and SPT locations are within 6 m of the V_S test locations; (4) at least two V_S measurements, and the corresponding test intervals, are within the uniform layer; (5) time history records used for V_S determination exhibit easy-to-pick shear-wave arrivals; and (6) all CPT measurements are made using electronic cone penetrometers. Where CPT measurements were not available, exceptions to Criterion 2 were allowed if there were at least three SPT blow counts that followed a consistent trend within the layer. When the time history records were not available, exceptions to Criterion 5 were allowed if three were at least 3 V_S measurements within the selected layer. By adopting these criteria, scatter in the data due to soil variability and measurement error is reduced.

Summarized in Tables 1–3 are the penetration resistance and V_S data pairs from Holocene, Pleistocene, and Tertiary sand deposits, respectively, with fines content (FC) less than 20%. Average values of median grain size (D_{50}) for the sand layers listed in the tables range from 0.15 to 0.86 mm. The sands classify as SP, SP-SM, SP-SC, SM, and SC by the Unified Soil Classification System.

Because soil samples are usually not collected during CPT investigations, the CPT-based soil behavior type index (I_c) by Robertson (1990) is also given in Tables 1–3 to characterize soil type. This index is computed by

$$I_c = [(3.47 - \log Q_t)^2 + (1.22 + \log F_N)^2]^{0.5} \quad (3)$$

where

$$Q_t = \left(\frac{q_t - \sigma_v}{P_a}\right)\left(\frac{P_a}{\sigma'_v}\right)^n \quad (4)$$

J. Geotech. Geoenviron. Eng., 2009, 135(6): 735-744

Table 2. Data from Pleistocene Sands with FC < 20% and $I_c < 2.25$ [Modified from Piratheepan (2002) and Ellis (2003)]

Site name	Depth (m)	USCS soil type	D_{50} (mm)	FC[a] (%)	V_S test type[b]	V_{S1} (m/s)	$(V_{S1})_{cs}$ (m/s)	$(N_1)_{60sc}$	I_c	q_{t1N}	$(q_{t1N})_{cs}$	Approximate average age[e] (years)
California, USA												
Oakland, USGS 45	3.9–7.7	na[c]	na	4[d]	SCPT	231	231	na	1.58	208	208	38 k(NL)
Oakland, USGS 53	6.1–9.4	na	na	9[d]	SCPT	270	278	na	1.84	225	256	38 k(NL)
Oakland, USGS 58	6.1–9.9	na	na	9[d]	SCPT	374	406	na	1.84	356	405	38 k(NL)
Alameda, USGS ALC021	4.0–12.0	na	na	5[d]	SCPT	248	249	na	1.66	262	265	38 k(NL)
Alameda, USGS ALC023	8.0–12.0	na	na	9[d]	SCPT	304	318	na	1.85	262	300	38 k(NL)
Alameda, USGS ALC025	8.0–12.0	na	na	9[d]	SCPT	279	289	na	1.86	207	239	38 k(NL)
Alameda, USGS ALC026	12.0–16.0	na	na	9[d]	SCPT	274	283	na	1.85	220	252	38 k(NL)
Alameda, USGS ALC029	4.0–10.0	na	na	8[d]	SCPT	238	242	na	1.81	220	245	38 k(NL)
Alameda, USGS ALC032	6.0–10.0	na	na	7[d]	SCPT	282	287	na	1.74	251	267	38 k(NL)
South Carolina, USA												
Charleston, S&ME 12	3.8–6.9	na	na	4[d]	SCPT	258	258	na	1.60	152	152	100 k(NL)
Charleston, WPC 42	8.7–10.7	na	na	6[d]	SCPT	242	243	na	1.70	90	93	100 k(NL)
James Island, WPC 37	1.7–3.7	SM	na	9[d]	SCPT	232	236	na	1.84	56	64	100 k(NL)
John's Island, WPC 53	1.4–4.4	na	na	11[d]	SCPT	248	255	na	1.91	83	100	100 k(NL)
John's Island, WPC 53	4.4–6.4	na	na	4[d]	SCPT	273	273	na	1.56	152	152	100 k(NL)
McClellanville, WPC 41	5.7–7.7	na	na	13[d]	SCPT	260	273	na	2.00	38	50	100 k(NL)
Mt. Pleasant, S&ME 7	13.5–18.5	na	na	15[d]	SCPT	238	249	na	2.08	50	71	100 k(NL)
Mt. Pleasant, WPC 1	3.4–6.4	na	na	7[d]	SCPT	194	195	na	1.74	108	115	100 k(NL)
Mt. Pleasant, WPC 28	2.0–5.0	na	na	12[d]	SCPT	259	270	na	1.92	115	139	100 k(NL)
Mt. Pleasant, WPC 45	3.7–5.7	SP	0.86	1	SCPT	283	283	na	1.38	239	239	100 k(NL)
Mt. Pleasant, WPC 38	2.4–5.0	na	na	4[d]	SCPT	243	243	na	1.57	171	171	100 k(NL)
Mt. Pleasant, WPC 54	2.9–5.9	na	na	10[d]	SCPT	244	250	na	1.89	83	98	100 k(NL)
No. Charleston, TEN-07	2.5–5.5	SP	na	16[d]	SCPT	204	210	9	2.10	62	91	110 (L)
No. Charleston, TEN-08	2.5–5.5	SP	na	15[d]	SCPT	186	190	11	2.06	62	86	110 (L)
No. Charleston, TEN-09	3.5–6.5	SP	na	18[d]	SCPT	168	171	9	2.18	50	81	110 (L)
No. Charleston, TEN-10	3.5–7.5	SP	na	18[d]	SCPT	169	172	8	2.18	50	81	110 (L)
No. Charleston, WPC 35	1.7–3.7	na	na	11[d]	SCPT	272	283	na	1.91	85	102	220 k(NL)
No. Charleston, WPC 43	3.6–5.6	na	na	16[d]	SCPT	194	198	na	2.10	51	74	115 (L)
No. Charleston, WPC 51	3.0—6.0	na	na	13[d]	SCPT	201	205	na	2.01	82	108	116 (L)

[a]FC=fines content (silt and clay).

[b]SCPT=seismic CPT.

[c]na=not available.

[d]Estimated fines content from: $FC = 1.75 I_c^{3.25} - 3.7$ for $1.26 < I_c < 3.5$ (Robertson and Wride 1998).

[e]Time between deposition (or liquefaction) and V_S measurements; L=known liquefaction; and NL=no known liquefaction; k=1,000.

$$F_N = \left(\frac{f_s}{q_t - \sigma_v} \right) 100\% \quad (5)$$

and where q_t=measured cone tip resistance (corrected for pore pressure acting behind the cone tip, if determined by piezocone); f_s=measured cone sleeve resistance; σ_v=in situ vertical total stress; σ'_v=vertical effective stress; P_a=reference stress of 100 kPa; and n=exponent that depends on soil type. The values of q_t, f_s, P_a, σ_v, and σ'_v are all in the same units. The value of n is about 0.5 for sand. According to Robertson and Wride (1998), sands with $I_c < 2.25$ typically have values of FC < 20%. The reason for selecting only sands with FC < 20% and $I_c < 2.25$ is to limit possible errors due to the equivalent clean sand corrections that are applied to the penetration resistance and V_S measurements, while providing a significant number of data pairs for analysis.

The approximate average ages given in Tables 1–3 are based on the number of years between the time of V_S measurements and the time of sand layer deposition or last known occurrence of liquefaction prior to V_S measurements. Grain-to-grain contacts are broken during liquefaction. As pore pressures dissipate, the contacts reform and the soil settles into a state that is denser than or just as loose as the state prior to shaking (Holzer and Youd 2007). The situation during liquefaction where pore pressure-induced seepage leads to localized loosening of the soil was described by Whitman (1985), and is often referred to as "void redistribution" (Idriss and Boulanger 2007). The reforming grain-to-grain contacts mark a resetting of the "aging clock" associated with the contacts. For this reason, the time between V_S measurements and liquefaction is given for some of the data as age of the deposit, even though the geologic age of original deposition is much older. Brief descriptions of the data pairs grouped by geologic age, as well as the equivalent clean sand corrections, are given below.

Holocene Data

The 22 Holocene data pairs (see Table 1) were originally published in Andrus et al. (2004a). They are presented in this paper with two modifications. The first modification is the addition of approximate average age of each sand layer. The second modifi-

J. Geotech. Geoenviron. Eng., 2009, 135(6): 735-744

Table 3. Data from Tertiary Sands with FC < 20% and $I_c < 2.25$ [Modified from Ellis (2003) and Lewis et al. (2008)]

Site name	Depth (m)	USCS soil type	D_{50} (mm)	FC[a] (%)	V_S test type[b]	V_{S1} (m/s)	$(V_{S1})_{cs}$ (m/s)	$(N_1)_{60cs}$	I_c	q_{t1N}	$(q_{t1N})_{cs}$	Approximate average age[e] (years)
South Carolina, USA												
Aiken, SRS 3 & 8	19.6–26.0	na	na	8[d]	SCPT	279	279	na	1.81	126	140	35 M(NL)
Aiken, SRS 5	20.5–26.9	na	na	6[d]	SCPT	262	264	na	1.69	104	107	35 M(NL)
Aiken, SRS 6	22.6–28.8	na	na	5[d]	SCPT	239	239	na	1.64	111	111	35 M(NL)
Aiken, SRS 7	21.4–26.7	na	na	6[d]	SCPT	271	272	na	1.68	119	122	35 M(NL)
Aiken, SRS 9	18.3–24.3	SP-SM	0.38	10	SCPT	256	261	31	1.81	86	96	35 M(NL)
Aiken, SRS 10	20.6–26.1	na	na	7[d]	SCPT	233	235	na	1.77	92	100	35 M(NL)
Aiken, SRS 13	21.5–27.9	na	na	5[d]	SCPT	269	270	na	1.66	107	108	35 M(NL)
Aiken, SRS 17	21.4–26.9	na	na	6[d]	SCPT	257	259	na	1.72	87	91	35 M(NL)
Aiken, Lewis 2	na[c]	SC	na	18.5	SCPT	268	294	na	2.19[d]	20	33	27 M(NL)
Aiken, Lewis 3	na	SP-SM	na	9.6	SCPT	255	262	na	1.87[d]	23	27	27 M(NL)
Aiken, Lewis 4	na	SC, SM, SP-SC	na	15.7	SCPT	257	274	na	2.10[d]	33	48	27 M(NL)
Aiken, Lewis 5	na	SP-SM, SC	na	10.8	SCPT	253	261	na	1.92[d]	50	60	27 M(NL)
Aiken, Lewis 10	na	SC	na	19.7	SCPT	162	165	na	2.22[d]	18	31	27 M(NL)
Aiken, Lewis 11	na	SC	na	16.1	SCPT	269	290	na	2.11[d]	19	28	35 M(NL)
Aiken, Lewis 12	na	SP-SC, SC	na	18.6	SCPT	206	213	na	2.19[d]	11	18	35 M(NL)

[a]FC=fines content (silt and clay).

[b]SCPT=seismic CPT.

[c]na=not available.

[d]Estimated fines content from: $FC = 1.75I_c^{3.25} - 3.7$ for $1.26 \leq I_c \leq 3.5$ (Robertson and Wride 1998).

[e]Time between deposition and V_S measurements; NL=no known liquefaction; and M=1,000,000.

cation is only 22 of the 43 original data pairs compiled by Andrus et al. (2004a) are listed in the table. The other 21 data pairs are not listed because the average age could not be reasonably approximated or the average fines content was >20% or the tip resistance was determined with a mechanical cone. Only 1 of the 43 original data pairs was based on the mechanical cone. Anagnostopoulos et al. (2003) showed significant difference in tip resistances measured by electronic and mechanical cones.

The Holocene data pairs are from sites in California (Mitchell et al. 1994; Boulanger et al. 2002; Fuhriman 1993; Hryciw 1991), Canada (Wride et al. 2000), and Japan (Iai, personal communication on sites in Hakodate Port, Japan, 1997; Iai et al. 1995). Of the 22 selected sites, 12 were tested by seismic cone, five by seismic crosshole, three by both seismic cone and crosshole, and two by suspension logger. Values of $(N_1)_{60}$ were determined from measured blow counts and reported test equipment and procedure information. Where energy measurements were not available, average corrections recommended by Youd et al. (2001) were assumed based on the type of hammer used. All of the CPT measurements are from 10 or 15 cm^2 cones. Values of q_{t1N} and I_c were averaged over the interval of the selected V_S measurements. When the electronic CPT data files were not available, average values were determined from the reported graphical profiles.

Pleistocene Data

The 28 Pleistocene data pairs (see Table 2) are from three named natural deposits in California and South Carolina. The three deposits are: (1) the Merritt Sand in Alameda and Oakland, California; (2) the Wando Formation in Charleston, South Carolina; and (3) the Ten Mile Hill beds also near Charleston. According to Helley and Graymer (1997), the Merritt Sand is between 6,000 and 71,000 years old. The Merritt Sand is a fine-grained, very well sorted wind-blown deposit. The U.S. Geological Survey (USGS) performed several seismic CPTs in the Merritt Sand as part of a liquefaction and ground shaking hazards mapping project (Holzer et al. 2002). Selected results from their tests are presented in Table 2.

The Wando Formation is 70,000 to 130,000 years old. As described by Weems and Lemon (1993), the Wando consists of only slightly weathered beds of sand, clayey sand, and clay. Evidence gathered on the Charleston peninsula indicates that little or no liquefaction occurred in the sand facies of the Wando during the 1886 Charleston earthquake (Hayati and Andrus 2008). Selected measurements from the sand facies of the Wando are listed in Table 2. The measurements are from various project reports by two engineering consulting firms based in Charleston, WPC, and S&ME.

The Ten Mile Hill beds are around 200,000 to 240,000 years old. As characterized by Weems and Lemon (1993), the Ten Mile Hill beds consist of sands, clayey sands, and clays deposited at a time when the sea level in the Charleston area stood about 11 m above its present level. Extensive liquefaction occurred in the Ten Mile Hill beds in the North Charleston areas during the 1886 earthquake. Selected measurements from the sand facies are listed in Table 2. These measurements are from the liquefaction study by Hu et al. (2002) and various project reports by WPC.

Shear-wave velocities in the 28 Pleistocene layers were determined by the seismic cone method. SPT measurements were available for four layers in the Ten Mill Hill beds (Hu et al. 2002). General procedures used for compiling the Pleistocene data were similar to procedures used for compiling the Holocene data.

Tertiary Data

The 15 Tertiary data pairs (see Table 3) are from the Tobacco Road and Dry Branch Formations beneath the Savannah River Site, South Carolina. The Tobacco Road is the younger of the two formations, dating at 25 to 29.5 million years before present (Christopher, personal communication on age of Dry Branch For-

mation, 2002). The Tobacco Road Formation exhibits characteristics similar to a low energy, shallow marine transitional environment, such as a tidal flat, and consists of sands with clay stringers and trace fossils (WSRC 2000).

The Dry Branch Formation dates around 34 to 36 million years before present (Christopher, personal communication on age of Dry Branch Formation, 2002). It has been characterized as a transitional sequence between near shore and bay to lagoon environments (WSRC 2000), which would be similar to the depositional environments of the Wando Formation and the Ten Mile Hill beds. Materials in the Dry Branch Formation classify as sand to clayey sand.

Selected penetration resistance-V_S data pairs from the Tobacco Road and Dry Branch Formations are given in Table 3. These data pairs were compiled from a project report by WSRC (2000) and a paper by Lewis et al. (2008). All of the 15 Tertiary data pairs were based on seismic cones. SPT measurements were available for one test location. General procedures used for compiling the Holocene data were followed for compiling the Tertiary data. Although the data from Lewis et al. (2008) do not satisfy general selection Criterion 4 (i.e., at least two V_S measurements and the corresponding test intervals are within the uniform layer), the data are believed to be of good quality.

Equivalent Clean Sand Corrections

Equivalent clean sand corrections to penetration resistance and V_S have been proposed to provide liquefaction evaluations that allow for continuous variations in fines content, rather than discrete limits (i.e., FC of 5, 15, and 35%). Robertson and Wride (1998) developed the following correction of the normalized CPT tip resistance q_{t1N} to an equivalent clean sand value:

$$(q_{t1N})_{cs} = K_c q_{t1N} = K_c (q_t/P_a)(P_a/\sigma'_v)^n \quad (6)$$

where $(q_{t1N})_{cs}$=equivalent clean sand value corresponding to q_{t1N}; and K_c=correction factor for fines content determined using the following relationships:

$$K_c = 1.0 \text{ for } I_c \leq 1.64 \quad (7a)$$

$$K_c = -0.403 I_c^4 + 5.581 I_c^3 - 21.63 I_c^2 + 33.75 I_c - 17.88 \text{ for } I_c > 1.64 \quad (7b)$$

I. M. Idriss with the assistance of R. B. Seed developed the following correction of the corrected SPT blow count $(N_1)_{60}$ to equivalent clean sand value (Youd et al. 2001):

$$(N_1)_{60cs} = \alpha + \beta (N_1)_{60} \quad (8)$$

where $(N_1)_{60cs}$=equivalent clean sand value corresponding to $(N_1)_{60}$; and α and β=coefficients determined using the following relationships:

$$\alpha = 0.0 \text{ for FC} \leq 5\% \quad (9a)$$

$$\alpha = e^{(1.76 - 190/\text{FC}^2)} \text{ for } 5\% < \text{FC} < 35\% \quad (9b)$$

$$\alpha = 5.0 \text{ for FC} \geq 35\% \quad (9c)$$

and

$$\beta = 1.0 \text{ for FC} \leq 5\% \quad (10a)$$

$$\beta = 0.99 + \text{FC}^{1.5}/1{,}000 \text{ for } 5\% < \text{FC} < 35\% \quad (10b)$$

$$\beta = 1.2 \text{ for FC} \geq 35\% \quad (10c)$$

For correcting normalized shear-wave velocity (V_{S1}) to an equivalent clean sand value, Juang et al. (2002) suggested the following correction:

$$(V_{S1})_{cs} = K_{cs} V_{S1} = K_{cs} V_S (P_a/\sigma'_v)^{0.25} \quad (11)$$

where $(V_{S1})_{cs}$=equivalent clean sand value corresponding to V_{S1}; and K_{cs}=correction factor for fines content determined using the following relationships:

$$K_{cs} = 1.0 \text{ for FC} \leq 5\% \quad (12a)$$

$$K_{cs} = 1 + (\text{FC} - 5)T \text{ for } 5\% < \text{FC} < 35\% \quad (12b)$$

$$K_{cs} = 1 + 30T \text{ for FC} \geq 35\% \quad (12b')$$

and

$$T = 0.009 - 0.0109(V_{S1}/100) + 0.0038(V_{S1}/100)^2 \quad (13)$$

As noted by Andrus and Stokoe (2000), application of Eq. (11) implicitly assumes a constant coefficient of earth pressure (horizontal effective stress divided by σ'_v) for all deposit types. It also assumes that V_S is measured with both the direction of particle motion and the direction of wave propagation polarized along principal stress directions and that one of those directions is vertical.

Eqs. (6)–(13) were used to convert measured penetration resistances and V_S measurements to the equivalent clean sand values listed in Tables 1–3. Where FC information was not available, an apparent FC value was computed using the average I_c value and a relationship suggested by Robertson and Wride (1998).

Holocene Penetration Resistance-V_S Relationships

To investigate the influence of age on penetration-V_S relationships, the regression equations proposed by Andrus et al. (2004a) for Holocene clean sands are used for reference. These equations are expressed as

$$(V_{S1})_{cs} = 87.8[(N_1)_{60cs}]^{0.253} \quad (14)$$

$$(V_{S1})_{cs} = 62.6[(q_{t1N})_{cs}]^{0.231} \quad (15)$$

where $(V_{S1})_{cs}$ in m/s, $(N_1)_{60cs}$ in blows/0.3 m, and $(q_{t1N})_{cs}$ is dimensionless. Eqs. (14) and (15) were derived using 36 and 39 data pairs from Holocene sand layers, respectively, including the data pairs listed in Table 1. As noted by Andrus et al. (2004a), Eq. (14) is most similar to relationships obtained by Yoshida et al. (1988) for fine sand, Fear and Robertson (1995) for Ottawa sand, and Andrus and Stokoe (2000) for uncemented, Holocene-age sands. Eq. (15) is most similar to the relationship by Robertson et al. (1992) for mainly quartz sands and Hegazy and Mayne (1995) for various sands. Combining Eqs. (14) and (15), one can obtain the following relationship (Andrus et al. 2004a):

$$(N_1)_{60cs} = 0.263[(q_{t1N})_{cs}]^{0.913} \quad (16)$$

Because Eqs. (14) and (15) were derived using data pairs from Holocene sand layers, Eq. (16) is also most appropriate for Holocene sands.

Plotted in Figs. 1–3 are the curves defined by Eqs. (14)–(16) along with the data pairs listed in Tables 1–3. It can be seen in the figures that the Holocene data points are fairly well distributed about the mean curves. On the other hand, the Pleistocene and

J. Geotech. Geoenviron. Eng., 2009, 135(6): 735-744

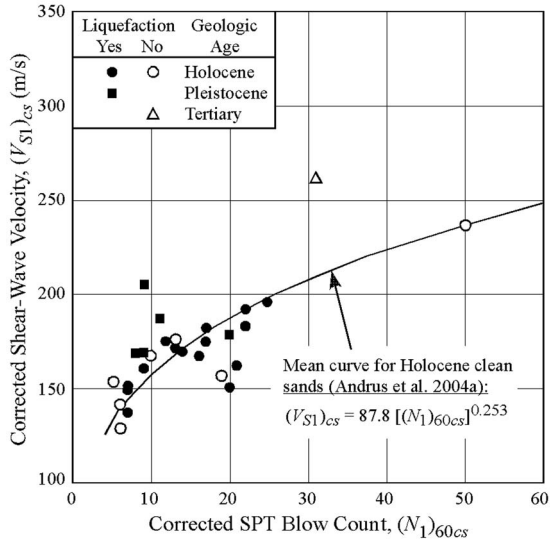

Fig. 1. Relationship between $(N_1)_{60cs}$ and $(V_{S1})_{cs}$ for uncemented, Holocene-age sands determined by Andrus et al. (2004a) with data from various sand deposits

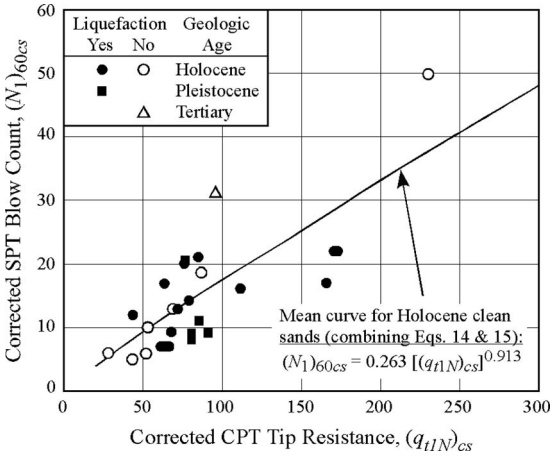

Fig. 3. Relationship between $(q_{t1N})_{cs}$ and $(N_1)_{60cs}$ for uncemented, Holocene-aged sands determined by Andrus et al. (2004a) with data from various sand deposits

Tertiary data generally plot above the curves in Figs. 1 and 2, suggesting that older soils generally exhibit higher shear-wave velocities than younger sands with similar penetration resistance. In Fig. 3, the plotted data are well distributed about the curve defined by Eq. (16).

Used also to investigate the influence of age on penetration resistance-V_S relationships is the equation proposed by Andrus et al. (2007, p. 6) for Holocene and Pleistocene soils. This equation adjusted for just Holocene soils is expressed as

$$V_{S1} = 17.2 q_{t1N}^{0.396} I_c^{1.006} \tag{17}$$

where V_{S1} in m/s, and q_{t1N} and I_c are dimensionless. Eq. (17) was determined using 72 Holocene data pairs and 113 Pleistocene data pairs, with I_c ranging from 1.2 to 4.0. Plotted in Fig. 4 are the curve defined by Eq. (17) and the CPT-V_S data pairs listed in Tables 1–3. It can be seen in Fig. 4 that the Holocene data generally have significantly lower values of V_S than the Pleistocene and Tertiary data pairs for the same penetration resistance.

Measured to Estimated Velocity Ratios

Plotted in Figs. 5 and 6 are values of MEVR and corresponding age for the data listed in Tables 1–3. The average age is taken as the time between soil deposition and V_S measurements for sites where no liquefaction has occurred. For sites where liquefaction has occurred, the average age is taken as the time between liquefaction occurrence and V_S measurements. It can also be seen in Figs. 5 and 6 that both liquefaction and no liquefaction data points plot within relatively narrow bands, whereas, if the older ages based on initial depositions were used, the scatter of data plotted in the figures would be much wider. Thus, these results

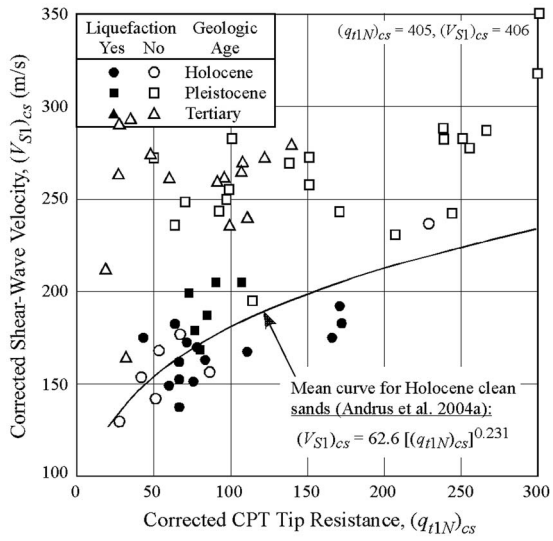

Fig. 2. Relationship between $(q_{t1N})_{cs}$ and $(V_{S1})_{cs}$ for uncemented, Holocene-age sands determined by Andrus et al. (2004a) with data from various sand deposits

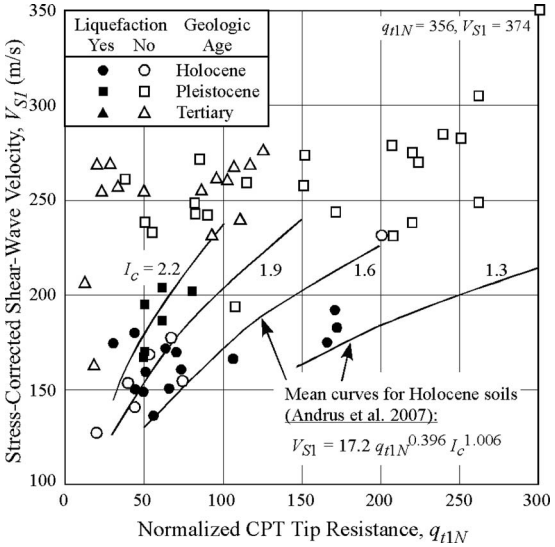

Fig. 4. Relationship between q_{t1N} and V_{S1} for uncemented, Holocene-age soils determined by Andrus et al. (2007) with data from various sand deposits

J. Geotech. Geoenviron. Eng., 2009, 135(6): 735-744

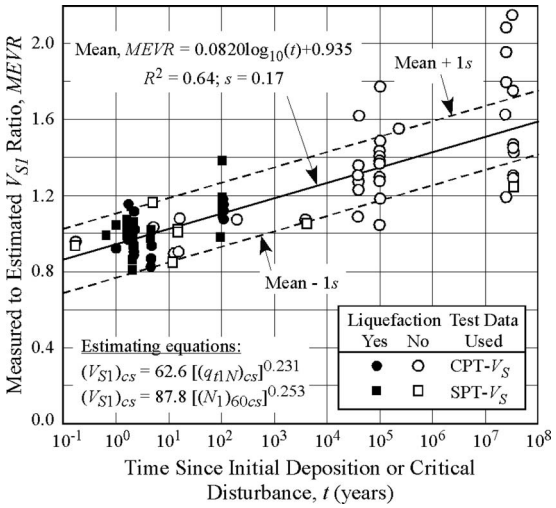

Fig. 5. Variation of measured to estimated V_{S1} ratio with time for sands based on the relationships by Andrus et al. (2004a)

shown in the figures provide evidence for the hypothesis that the "aging clock" of sand deposits is reset to zero time during liquefaction.

In Fig. 5, values of MEVR are based on Eqs. (14) and (15). The regression line shown in the figure can be expressed as

$$\text{MEVR} = 0.0820 \log_{10}(t) + 0.935 \tag{18}$$

The coefficient of determination (R^2) and standard deviation of the residuals or errors (s) associated with this regression equation are 0.64 and 0.17, respectively. Eq. (18) suggests that MEVR increases by a factor of about 0.082 each log cycle of time. Eq. (18) provides $t=6.2$ years for MEVR=1.0, suggesting 6.2 years for an approximate average age of sand layers used to develop Eqs. (14) and (15).

In Fig. 6, plotted values of MEVR are based on Eq. (17). The regression line shown in the figure can be expressed as

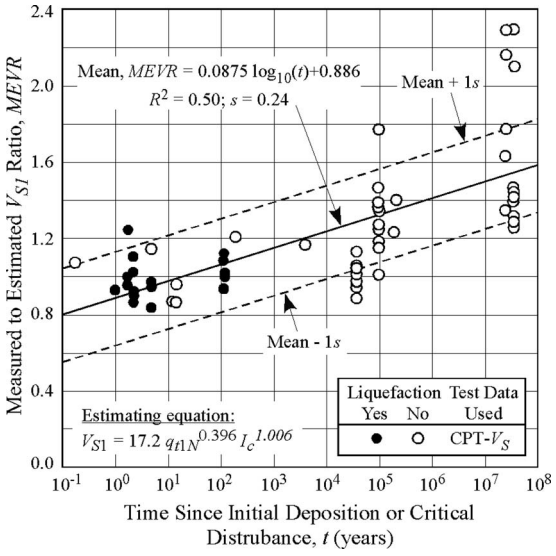

Fig. 6. Variation of measured to estimated V_{S1} ratio with time for sands based on the relationships by Andrus et al. (2007)

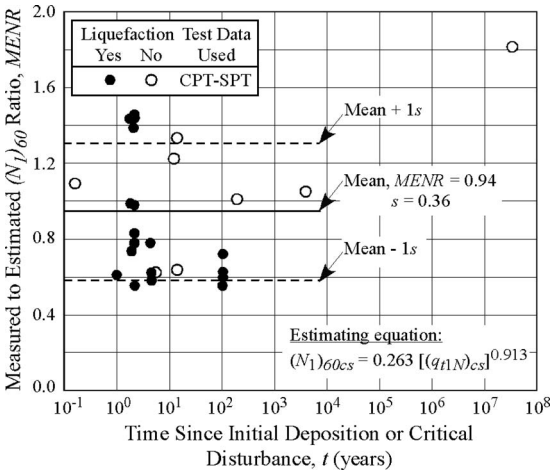

Fig. 7. Variation of measured to estimated $(N_1)_{60}$ ratio with time for sands based on the relationships by Andrus et al. (2004a)

$$\text{MEVR} = 0.0875 \log_{10}(t) + 0.886 \tag{19}$$

Values of R^2 and s associated with this regression equation are 0.50 and 0.24, respectively. Eq. (19) suggests that MEVR increases by a factor of about 0.0875 for each log cycle of time, and provides $t=20$ years at MEVR of 1.0. These results agree well with Eq. (18).

To evaluate the appropriateness of mixing CPT and SPT data, ratios of measured $(N_1)_{60}$ to estimated $(N_1)_{60}$ are calculated using Eq. (16). These ratios, herein called MENR, are plotted versus time in Fig. 7. The plotted values of MENR exhibit significant scatter and no distinct trend with time can be justified. The mean MENR of 0.94 suggests that $(N_1)_{60}$ might be slightly underestimated by Eq. (15) on average. However, the large s value of 0.36 and no distinct trend with time indicate that both $(N_1)_{60}$ and q_{t1N} may be similarly influenced by age. Thus, the mixing CPT- and SPT-based data should not have a significant impact on Eq. (18).

The findings of this section indicate that the penetration-V_S relationships represented by Eqs. (14), (15), and (17) are specifically for young sand deposits 6–20 years old. The MEVR values agree with the previous work of Ohta and Goto (1978), who suggested an average of 1.00 for Holocene-age soils and 1.30 for Pleistocene-age soils. Eqs. (18) and (19) provide MEVR of 1.34 and 1.32, respectively, for an average Pleistocene age of 100,000 years. Eq. (18) is preferred because of the higher R^2 and the lower s associated with its regression. Multiplying Eqs. (14) and (15) by Eq. (18), one can obtain the following relationships:

$$(V_{S1})_{cs} = [7.20 \log_{10}(t) + 82.1][(N_1)_{60cs}]^{0.253} \tag{20}$$

$$(V_{S1})_{cs} = [5.13 \log_{10}(t) + 58.5][(q_{t1N})_{cs}]^{0.231} \tag{21}$$

Eqs. (20) and (21) are the recommended penetration resistance-V_S relationships in sands with little or no cementation.

Liquefaction Resistance Curves for Aged Sands

Andrus et al. (2004a) used Eqs. (14) and (15) to show that there is good general agreement between liquefaction resistance curves based on SPT, CPT, and V_S for young sands (say 1 to 20 years old, the range of many liquefaction case histories). For older sands, however, V_S is more sensitive to age and cementation than SPT blow count and CPT tip resistance. Thus, without an age

J. Geotech. Geoenviron. Eng., 2009, 135(6): 735-744

Table 4. Correction Factors for Evaluating Liquefaction Resistance of Sands

Time since initial deposition or critical disturbance, t (years)	Measure to estimated V_S ratio, MEVR [Eq. (18)]	Deposit resistance correction factor, K_{DR} [Eq. (2)]
0.1	0.85	0.66
1	0.94	0.83
10	1.02	1.00
100	1.10	1.17
1,000	1.18	1.34
10,000	1.26	1.51
100,000	1.34	1.68
1,000,000	1.43	1.85
10,000,000	1.51	2.02

correction to V_S, it is likely that liquefaction potential evaluations with V_S will be less conservative in aged sands. The variable MEVR and Eq. (18) provide a way of adjusting V_S to be the young age associated with Eqs. (14) and (15).

For liquefaction resistance predictions in Holocene soils with V_S, it has been proposed that CRR be defined as [modified from Andrus and Stokoe (2000); Andrus et al. (2004b)]

$$\mathrm{CRR}_{7.5y} = 0.022\left(\frac{V_{S1}}{100\mathrm{MEVR}}\right)^2 + 2.8\left(\frac{1}{V_{S1}^* - V_{S1}/\mathrm{MEVR}} - \frac{1}{V_{S1}^*}\right) \tag{22}$$

where $\mathrm{CRR}_{7.5y}$=cyclic resistance ratio for young soil deposits and earthquakes with moment magnitude (M_w) of 7.5, and V_{S1}^* =limiting upper value of V_{S1} for liquefaction occurrence. Andrus and Stokoe (2000) suggested V_{S1}^*=215 m/s for FC≤5%; V_{S1}^* =215−0.5(FC−5) m/s for 5%<FC<35%; V_{S1}^*=200 m/s for FC≥35%. Juang et al. (2002) characterized Eq. (22) as a 26% probability of liquefaction (P_L) relationship using logistic regression and Bayesian mapping techniques. The relationship between P_L and factor of safety against liquefaction (F_S) using Eq. (22) can be expressed as

$$P_L = 1/[1 + (F_S/0.73)^{3.4}] \tag{23}$$

where F_S is defined as CRR divided by CSR.

Recommended values of MEVR and K_{DR} based on Eqs. (18) and (2), respectively, are tabulated in Table 4. Because both variables are functions of $\log_{10}(t)$ and for sands, Eqs. (18) and (2) can be combined to obtain

$$K_{DR} = 2.07\mathrm{MEVR} - 1.11 \tag{24}$$

Eq. (24) provides a practical alternative to the often difficult problem of determining age of a deposit.

Eq. (24) can be used for correcting the V_S-based CRR curve, as well as the SPT- and CPT-based CRR curves. Plotted in Figs. 8–10 are the clean sands (i.e., FC≤5%), $\mathrm{CRR}_{7.5}$ curves based on V_{S1}, $(N_1)_{60}$, and q_{t1N}, respectively, for various values of MEVR. The V_{S1}-based curves shown in Fig. 8 are derived using Eqs. (1), (18), (22), and (24), and adjusted to a probability of liquefaction (P_L) of 30% using Eq. (23). The V_{S1}-based CRR curves indicate the effect of age is negligible below V_{S1} of about 150 m/s. The effect is negligible below V_{S1} of about 150 m/s because the MEVR corrections to V_{S1} and CRR practically cancel each other out. Above V_{S1} of 150 m/s, the curves suggest limiting upper

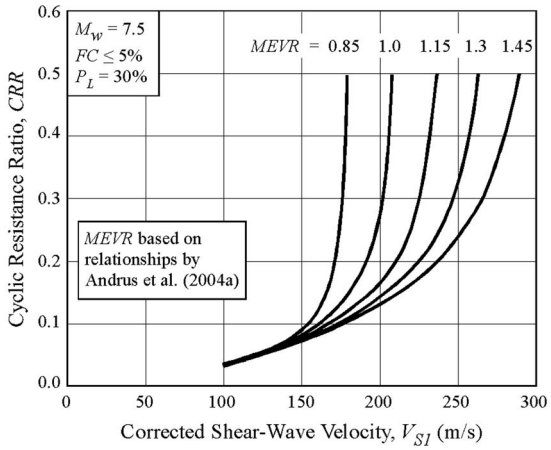

Fig. 8. CRR curves based on V_{S1} for clean sands and magnitude 7.5 earthquakes corrected for age

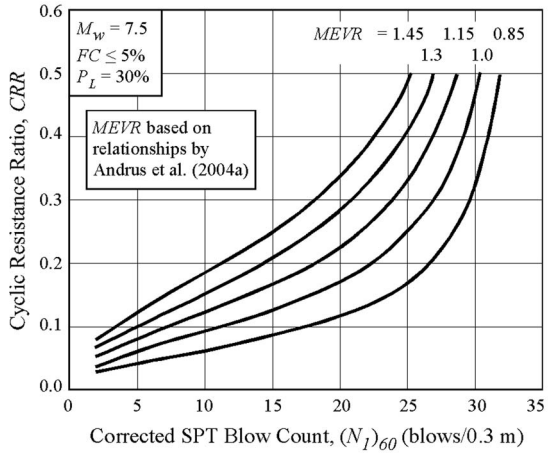

Fig. 9. CRR curves based on $(N_1)_{60}$ for clean sands and magnitude 7.5 earthquakes corrected for age

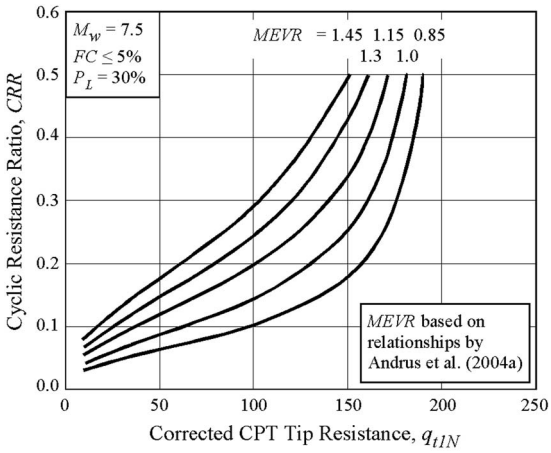

Fig. 10. CRR curves based on q_{t1N} for clean sands and magnitude 7.5 earthquakes corrected for age

J. Geotech. Geoenviron. Eng., 2009, 135(6): 735-744

bound values of V_{S1} for liquefaction occurrence ranging from 180 m/s to 290 m/s for MEVR of 0.85 to 1.45, respectively. This trend is opposite from the trend suggested by the age-corrected CRR curves proposed by Leon et al. (2006). The CRR curve for MEVR of 1.0 and P_L=30% in Fig. 8 lies slightly above the deterministic curve proposed by Andrus and Stokoe (2000) defined by Eq. (22).

The $(N_1)_{60}$- and q_{t1N}-based CRR curves shown in Figs. 9 and 10 are derived using the same procedure used to derive the curves shown in Fig. 8, except Eqs. (14) and (15), respectively, are substituted for V_{S1} in Eq. (22). The CRR curves shown in the figures indicate that liquefaction resistance increases significantly with increasing MEVR. This trend generally agrees with trends suggested by Lewis et al. (2004) and Leon et al. (2006). The curves for MEVR of 1.0 and P_L=30% in Figs. 9 and 10 lie slightly above the curves derived by Andrus et al. (2004a) based on Eqs. (14) and (15).

When applying the liquefaction evaluation curves shown in Figs. 8–10 for design, a F_S of 1.2 to 1.5 should be used (BSSC 2000; Juang et al. 2002; Andrus et al. 2004b). It should also be noted that only CRR and V_S are corrected for age. The correction applied to V_S is to account for the fact that V_S is more sensitive to age than penetration resistance. The $(N_1)_{60}$ and q_{t1N} values are not corrected for age to be consistent with the assumption made in the development of K_{DR} [see Eq. (2)].

Although it has been shown that SPT blow counts or CPT tip resistances divided by relative densities increase with age (Skempton 1986; Kulhawy and Mayne 1990), Eq. (2) was derived assuming commonly used CRR curves as reference (Youd et al. 2001). That is, values of K_{DR} were computed by dividing the measured CRR by the reference CRR for the given penetration resistance uncorrected for age (Hayati et al. 2008). Two major advantages of this approach are: (1) the K_{DR} correction is directly applied to the well-established commonly used CRR curves; and (2) the uncertainty and error associated with correcting penetration resistance for age are not introduced into the K_{DR} correction. Thus, the influence of age on the SPT- and CPT-based CRR curves shown in Figs. 9 and 10, respectively, is adequately addressed.

Conclusions

The influence of age on penetration resistance-V_S relationships was quantified using 64 CPT-V_S and 27 SPT-V_S data pairs from sand layers ranging in age from 0.2 years to 35 million years. For reference, the penetration resistance-V_S relationships proposed by Andrus et al. (2000a, 2007) for Holocene soils were considered. Ratios of measured V_S to estimated V_S (called MEVR) were computed for each data pair. Linear regressions of MEVR versus time indicate that MEVR increases by a factor of about 0.08 per $\log_{10}$ cycle of time.

Eq. (18), the recommended time-MEVR relationship, was combined with the time-deposit resistance correction factor relationship derived by Hayati et al. (2008) to obtain the relationship given in Eq. (24). Eq. (24) was in turn used to create corrected CRR curves based on V_{S1}, $(N_1)_{60}$, and q_{t1N} for various values of MEVR. These new CRR curves are recommended for evaluating liquefaction potential of sands of all ages (or MEVRs).

Because the age-corrected CRR curves are based on data from clean sands and silty sands, greater care should be exercised when applying the curves to other soil types. Additional penetration resistance-V_S data are needed from all deposit types and ages to further validate and extend the results of this study.

Acknowledgments

This research was supported by the National Science Foundation (NSF) under Grant No. CMS-0556006. Previous support for data compilation was provided by the U.S. Geological Survey (USGS), Department of the Interior under USGS Award Nos. 01HQGR007 and 05HQGR0037, and by the South Carolina Department of Transportation (SCDOT) and the Federal Highway Administration (FHWA) under SCDOT Research Project No. 623. Any opinions, findings, and conclusions or recommendations expressed in this material are those of the writers and do not necessarily reflect the views of NSF, USGS, SCDOT, or FHWA. The writers express their sincere thanks to these organizations, as well as to the many individuals who generously assisted with data compilation. In particular, T. L. Holzer, M. J. Bennett, J. C. Tinsley, III, and T. E. Noce of USGS; T. J. Casey and W. B. Wright of WPC; S. L. Gassman of the University of South Carolina; F. Syms and D. Wyatt of Bechtel Savannah River, Inc; W. M. Camp and T. J. Cleary of S&ME; T. N. Adams of SCDOT; and P. Piratheepan, B. S. Ellis, J. Zhang, A. Shrikhande, and C. D. Fairbanks, former graduate students at Clemson University.

References

Anagnostopoulos, A., Koukis, G., Sabatakakis, N., and Tsiamboas, G. (2003). "Empirical correlation of soil parameters based on cone penetration tests (CPT) for Greek soils." *Geotech. Geologic. Eng.*, 21(4), 377–387.

Andrus, R. D., Mohanan, N. P., Piratheepan, P., Ellis, B. S., and Holzer, T. L. (2007). "Predicting shear-wave velocity from cone penetration resistance." *Proc., Earthquake Geotechnical Engineering, 4th Int. Conf. on Earthquake Geotechnical Engineering—Conf. Presentations* (CD-ROM), K. D. Pitilakis, ed., Springer, The Netherlands, Paper No. 1454.

Andrus, R. D., Piratheepan, P., Ellis, B. S., Zhang, J., and Juang, C. H. (2004a). "Comparing liquefaction evaluation methods using penetration-V_S relationships." *Soil Dyn. Earthquake Eng.*, 24(9–10), 713–721.

Andrus, R. D., and Stokoe, K. H., II (2000). "Liquefaction resistance of soils from shear-wave velocity." *J. Geotech. Geoenviron. Eng.*, 126(11), 1015–1025.

Andrus, R. D., Stokoe, K. H., II, and Juang, C. H. (2004b). "Guide for shear wave-based liquefaction potential evaluation." *Earthquake Spectra*, 20(2), 285–308.

Arango, I., Lewis, M. R., and Kramer, C. (2000). "Updated liquefaction potential analysis eliminates foundation retrofitting of two critical structures." *Soil Dyn. Earthquake Eng.*, 20, 17–25.

Arango, I., and Migues, R. E. (1996). "Investigation of the seismic liquefaction of old sand deposits." *Rep. on Research*, Bechtel Corp., National Science Foundation Grant No. CMS-94–16169, San Francisco, Calif.

Boulanger, R. W., Mejia, L. H., and Idriss, I. M. (2002). "Liquefaction at Moss Landing during Loma Prieta earthquake." *J. Geotech. Geoenviron. Eng.*, 123(5), 453–467.

Building Seismic Safety Council (BSSC). (2000). "NEHRP recommended provisions for seismic regulation for new buildings and other structures." *FEMA, 368*, Federal Emergency Management Agency, Washington, D.C., Part 2.

Ellis, B. S. (2003). "Regression equations for estimating shear-wave velocity in South Carolina sediments using penetration test data." MS thesis, Clemson Univ., Clemson, S.C.

Fear, C. E., and Robertson, P. K. (1995). "Estimating the undrained strength of sand: A theoretical framework." *Can. Geotech. J.*, 32, 859–870.

Fuhriman, M. D. (1993). "Crosshole seismic tests at two northern California sites affected by the 1989 Loma Prieta earthquake." MS thesis, Univ. of Texas at Austin, Austin, Tex.

Hayati, H., and Andrus, R. D. (2008). "Liquefaction potential map of Charleston, South Carolina based on the 1886 earthquake." *J. Geotech. Geoenviron. Eng.*, 134(6), 815–828.

Hayati, H., Andrus, R. D., Gassman, S. L., Hasek, M., Camp, W. M., and Talwani, P. (2008). "Characterizing the liquefaction resistance of aged soils." *Proc., Geotechnical Earthquake Engineering and Soil Dynamics IV*, 1–10.

Hegazy, Y. A., and Mayne, P. W. (1995). "Statistical correlations between V_S and cone penetration data for different soil types." *Proc., Int. Symp. on Cone Penetration Testing, CPT '95*, 2, 173–178.

Helley, E. J., and Graymer, R. W. (1997). "Quaternary geology of Alameda County, and parts of Contra Costa, Santa Clara, San Mateo, San Francisco, Stanislaus, and San Joaquin counties, California: A digital database." *U.S. Geological Survey Open-File Rep. No. 97-097*.

Holzer, T. L., Bennett, M. J., Noce, T. E., Padovani, A. C., and Tinsley, J. C., III (2002). "Liquefaction hazard and shaking amplification maps of Alameda, Berkeley, Emeryville, Oakland, and Piedmont: A digital database." *U.S. Geological Survey Open-File Rep. No. 02-296* ⟨http://geopubs.wr.usgs.gov/open-file/of02-296⟩.

Holzer, T. L., and Youd, T. L. (2007). "Liquefaction, ground oscillation, and soil deformation at the Wildlife Array, California." *Bull. Seismol. Soc. Am.*, 97(3), 961–976.

Hryciw, R. D. (1991). "Post Loma Prieta earthquake CPT, DMT and shear wave velocity investigations of liquefaction sites in Santa Cruz and on Treasure Island." *Final Rep. to the U. S. Geological Survey, Award No. 14-08-0001-G1865*, Univ. of Michigan at Ann Arbor.

Hu, K., Gassman, S. L., and Talwani, P. (2002). "In-situ properties of soils at paleoliquefaction sites in the South Carolina coastal plain." *Seismol. Res. Lett.*, 73(6), 964–978.

Iai, S., Morita, T., Kameoka, T., Matsunaga, Y., and Abiko, K.. (1995). "Response of a dense sand deposit during 1993 Kushiro-Oki earthquake." *Soils Found.*, 35(1), 115–131.

Idriss, I. M., and Boulanger, R. W. (2007). "SPT- and CPT-based relationships for the residual shear strength of liquefied soils." *Earthquake geotechnical engineering*, K. D. Pitilalis, ed., Springer, The Netherlands, 1–22.

Juang, C. H., Jiang, T., and Andrus, R. D., (2002). "Assessing probability-based methods for liquefaction potential evaluation." *J. Geotech. Geoenviron. Eng.*, 128(7), 580–589.

Kulhawy, F. H., and Mayne, P. W. (1990). "Manual on estimating soil properties for foundation design." *Final Rep. No. 1492-6, EL-6800*, Electric Power Research Institute, Palo Alto, Calif.

Leon, E., Gassman, S. L., and Talwani, P. (2006). "Accounting for soil aging when assessing liquefaction potential." *J. Geotech. Geoenviron. Eng.*, 132(3), 363–377.

Lewis, M. R., Arango, I., Kimball, J. K., and Ross, T. E. (1999) "Liquefaction resistance of old sand deposits." *Proc., 11th Panamerican Conf. on Soil Mechanics and Geotechnical Engineering*, 821–829.

Lewis, M. R., Arango, I., and McHood, M. D. (2008). "Site characterization philosophy and liquefaction evaluation of aged sands —A Savannah river Site and Bechtel Perspective." *From research to practice, geotechnical special publication No. 180*, J. E. Laaaier, D. K. Crapps, and M. H. Hussein, eds., 540–558.

Lewis, M. R., McHood, M. D., and Arango, I. (2004). "Liquefaction evaluations at the Savannah River Site, a case history." *Proc., Fifth Int. Conf. on Case Histories in Geotechnical Engineering*, Paper No. 3.21.

Mitchell, J. K. et al. (1994). "In situ test results from four Loma Prieta earthquake liquefaction sites: SPT, CPT, DMT, and shear wave velocity." *Report No. UCB/EERC-09/04*, Earthquake Engineering Research Center, Univ. of California at Berkeley.

Mohanan, N. (2006). "Evaluation of shear wave velocity-cone penetration resistance regression equations based on geology for Charleston, South Carolina." MS thesis, Clemson Univ., Clemson, S.C.

Ohta, Y., and Goto, N. (1978). "Empirical shear wave velocity equations in terms of characteristic soil indexes." *Earthquake Eng. Struct. Dyn.*, 6, 167–187.

Piratheepan, P. (2002). "Estimating shear-wave velocity from SPT and CPT data." MS thesis, Clemson Univ., Clemson, S.C.

Robertson, P. K. (1990). "Soil classification using the cone penetration test." *Can. Geotech. J.*, 27, 151–158.

Robertson, P. K., et al. (2000). "The CANLEX project: Summary and conclusions." *Can. Geotech. J.*, 37, 563–591.

Robertson, P. K., Woeller, D. J., and Finn, W. D. L. (1992). "Seismic CPT for evaluating liquefaction potential." *Can. Geotech. J.*, 29, 686–695.

Robertson, P. K., and Wride, C. E. (1998). "Evaluating cyclic liquefaction potential using the cone penetration test." *Can. Geotech. J.*, 35(3), 442–459.

Seed, H. B. (1979). "Soil liquefaction and cyclic mobility evaluation for level ground during earthquakes." *J. Geotech. Engrg. Div.*, 105(2), 201–255.

Seed, H. B., and Idriss, I. M. (1971). "Simplified procedure for evaluating soil liquefaction potential." *J. Soil Mech. and Found. Div.*, 97(9), 1249–1273.

Skempton, A. W. (1986). "Standard penetration test procedures and the effects in sands of overburden pressure, relative density, particle size, ageing and overconsolidation." *Geotechnique*, 36(3), 425–447.

Troncoso, J., Ishihara, K., and Verdugo, R. (1988). "Aging effects on cyclic shear strength of tailing materials." *Proc., 9th World Conf. on Earthquake Engineering*, Vol. III, 121–126.

Weems, R. E., and Lemon, E. M., Jr. (1993). "Geology of the Cainhoy, Charleston, Fort Moultrie, and North Charleston quadrangles, Charleston and Berkeley counties, South Carolina." *USGS Miscellaneous Investigation Map I-1935*, Scale 1:24,000, U.S. Geological Survey, Reston, Va.

Westinghouse Savannah River Corp. (WSRC). (2000). "CPTu-$(N_1)_{60}$ determination." *WSRC Rep. No. K-CLC-G-00067*, Westinghouse Savannah River Corporation, Aiken, S.C.

Whitman, R. V. (1985). "On liquefaction." *Proc., 11th Int. Conf. on the Soil Mechanics and Foundation Engineering*, Balkema, Rotterdam, The Netherlands, 1923–1926.

Wride (Fear), C. E. et al. (2000). "Interpretation of in situ test results from the CANLEX sites." *Can. Geotech. J.*, 37, 505–529.

Yoshida, Y., Ikemi, M., and Kokusho, T. (1988). "Empirical formulas of SPT blow counts for gravelly soils." *Proc., Penetration Testing 1988, ISOPT-1*, Vol. 2, 381–387.

Youd, T. L., et al. (2001). "Liquefaction resistance of soils: Summary report from the 1996 NCEER and 1998 NCEER/NSF workshops on evaluation of liquefaction resistance of soils." *J. Geotech. Geoenviron. Eng.*, 127(10), 817–833.

Youd, T. L., and Perkins, D. M. (1978). "Mapping of liquefaction induced ground failure potential." *J. Geotech. Engrg. Div.*, 104(4), 433–446.

J. Geotech. Geoenviron. Eng., 2009, 135(6): 735-744